Electronic Supplementary Material (ESI) for Dalton Transactions
This journal is © The Royal Society of Chemistry 2012

Supporting Information

A joint application of spectroscopic, electrochemical and theoretical approaches in evaluation of the radical scavenging activity of 3-OH flavones and their iron complexes towards different radical species

Jasmina M. Dimitrić Marković*[a], Zoran S. Marković[b], Igor A. Pašti[a], Tanja P. Brdarić[c], Ana Popović Bijelić[a], Miloš Mojović [a]

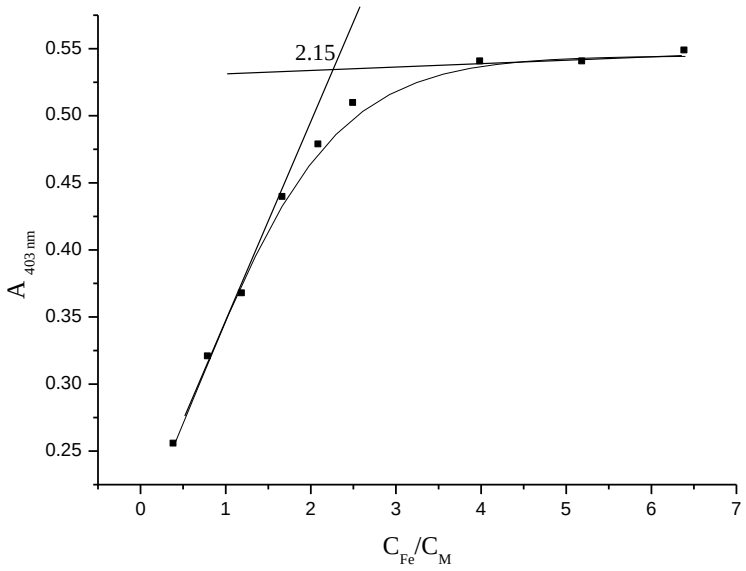

Fig. S1 Complex absorbance at 420 nm *versus* [Fe]/[M] concentrations

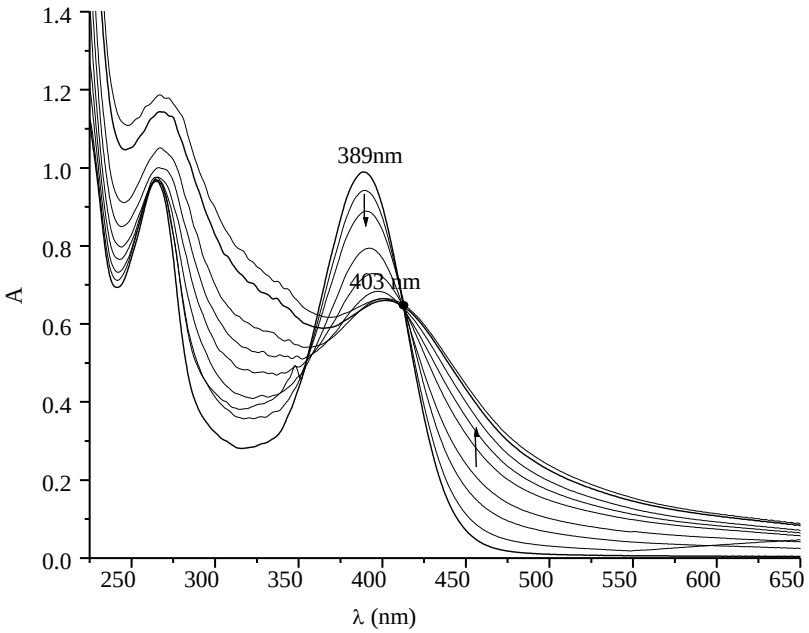

Fig. S2 Titration curves of morin with iron(III) at pH 7

This journal is © The Royal Society of Chemistry 2012

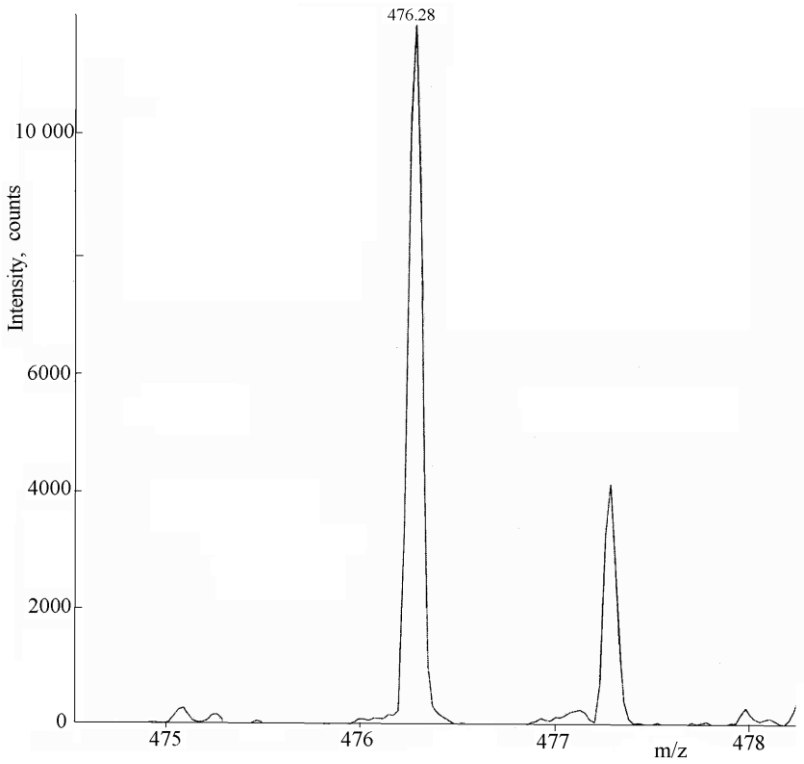

a)

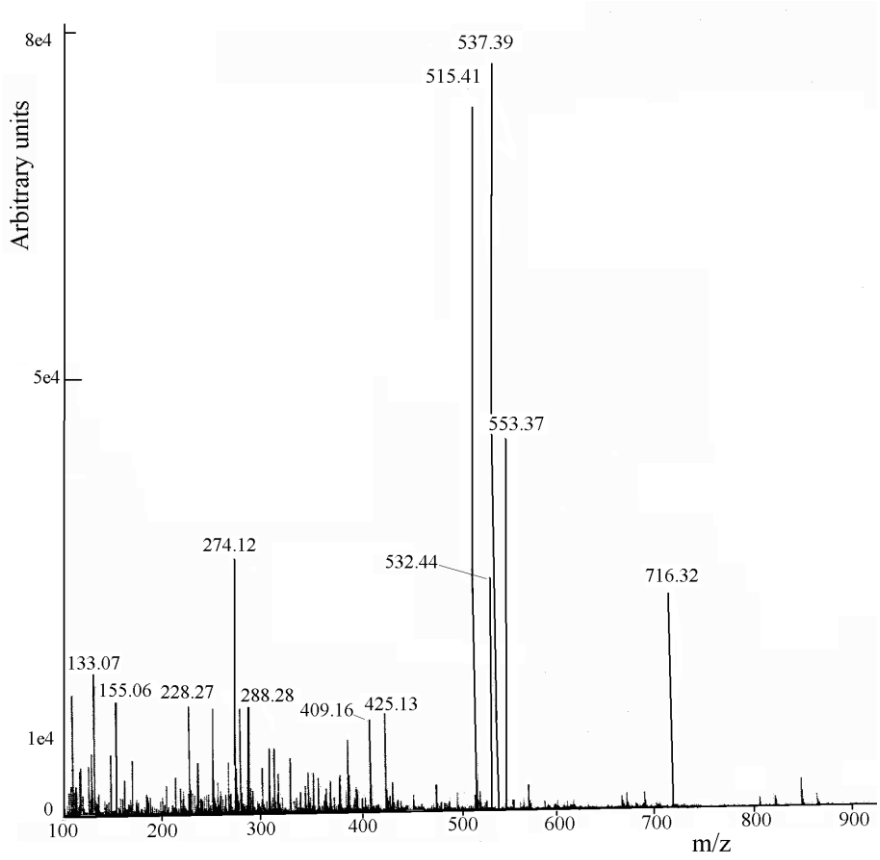

b)

Fig. S3 Isotopic pattern of the peak at m/z = 476.28 (a) MS spectra of MeOH-H_2O (1:1) mixture (b)

This journal is © The Royal Society of Chemistry 2012

Table S1
Bond lengths (in Å) calculated for morin and corresponding iron complex

Bond lengths	X ray*	M052X/6-311G(d,p)	Iron(II)-morin complex (2:1)
C(2)-O(1)	1.375	1.365	1.340
C(2)-C(3)	1.355	1.352	1.406
C(2)-C(1')	1.464	1.462	1.432
C(3)-C(4)	1.455	1.444	1.393
C(3)-O(3)	1.372	1.365	1.355
O(3)-- Fe			1.822
Fe—OH-Me			1.942
C(4)-C(10)	1.438	1.433	1.410
C(4)-O(4)	1.258	1.244	1.366
C(10)-C(5)	1.425	1.415	1.428
C(10)-C(9)	1.396	1.400	1.414
C(5)-C(6)	1.368	1.382	1.382
C(5)-O(5)	1.348	1.334	1.325
O(5)-- Fe			1.800
Fe—OH-Me			1.953
C(6)-C(7)	1.410	1.398	1.401
C(7)-C(8)	1.396	1.390	1.394
C(7)-O(7)	1.349	1.350	1.331
C(8)-C(9)	1.386	1.382	1.372
C(9)-O(1)	1.369	1.355	1.356
C(l')-C(2')	1.404	1.407	1.426
C(2')-C(3')	1.394	1.393	1.386
C(2')-O(2')	1.370	1.347	1.338
C(3')-C(4')	1.376	1.384	1.387
C(4')-C(5')	1.394	1.397	1.410
C(4')-0(4')	1.372	1.355	1.329
C(5')-C(6')	1.378	1.375	1.360
C(l')-C(6')	1.403	1.405	1.427
O(2')-H(2')	1.000	0.970	0.982
O(4')-H(4')	0.913	0.959	0.962
O(3)-H(3)	0.845	0.970	
O(5)-H(5)	0.912	0.979	
O(7)-H(7)	0.877	0.960	0.962
O(2')-H(2')---O(3)	1.739	1.735	1.566
O(3)-H(3)---O(4)	2.287	2.031	
O(5)-H(5)---O(4)	1.832	1.782	

* Data taken from ref. [28]

This journal is © The Royal Society of Chemistry 2012

Table S2
Bond angles and dihedral angles (in ^{o}) for morin and corresponding iron complex

Angles	X ray*	M052X/6-311 G (d,p)	Iron(II)-morin complex (2:1)
0(l)-C(2)-C(3)	120.40	119.588	116.327
O(l)-C(2)-C(1')	111.20	112.127	112.831
C(3)-C(2)-C(l')	128.30	128.249	130.805
C(2)-C(3)-C(4)	121.90	122.230	120.490
C(2)-C(3)-O(3)	120.20	122.748	123.087
C(4)-C(3)-O(3)	117.70	115.020	116.313
C(3)-O(3)--Fe			110.678
O(3)--Fe-- OH-Me			99.352
C(3)-C(4)-C(10)	115.60	115.896	121.710
C(3)-C(4)-O(4)	120.10	119.000	114.628
C(10)-C(4)-O(4)	124.30	125.086	123.654
C(4)-C(10)-C(5)	122.30	121.715	126.751
C(4)-C(10)-C(9)	119.90	119.468	115.767
C(5)-C(10)-C(9)	117.80	118.811	117.398
C(10)-C(5)-C(6)	120.30	119.672	119.310
C(10)-C(5)-O(5)	120.00	120.758	121.572
C(6)-C(5)-O(5)	119.60	119.570	119.111
C(5)-O(5)--Fe			125.765
O(5)--Fe-- OH-Me			93.815
C(5)-C(6)-C(7)	119.90	119.564	120.927
C(6)-C(7)-C(8)	121.60	122.158	121.139
C(6)-C(7)-O(7)	121.30	121.170	122.441
C(8)-C(7)-O(7)	117.10	116.672	116.418
C(7)-C(8)-C(9)	117.10	117.611	117.648
0(l)-C(9)-C(10)	121.20	120.675	119.997
O(l)-C(9)-C(8)	115.50	117.141	116.440
C(10)-C(9)-C(8)	123.30	122.183	123.555
C(2)-C(l')-C(2')	123.90	123.808	126.011
C(2)-C(l')-C(6')	118.50	117.950	116.824
C(l')-C(2')-C(3')	120.60	119.635	120.134
C(l')-C(2')-O(2')	122.50	124.376	124.004
C(3')-C(2')-0(2')	116.80	115.905	115.807
C(2')-C(3')-C(4')	120.10	120.796	120.854
C(3')-C(4')-C(5')	120.60	120.375	120.310
C(3')-C(4')-O(4')	122.00	122.256	123.163
C(5')-C(4')-O(4')	117.30	117.369	116.525
C(4')-C(5')-C(6')	119.00	118.780	119.074
C(l')-C(6')-C(5')	122.10	122.279	122.627
C(2)-O(l)-C(9)	120.80	122.089	125.640
t(C(3)-C(2)-C(1`)-C(2`))	43.4	38.269	23.90

* Data taken from ref. [28]

This journal is © The Royal Society of Chemistry 2012

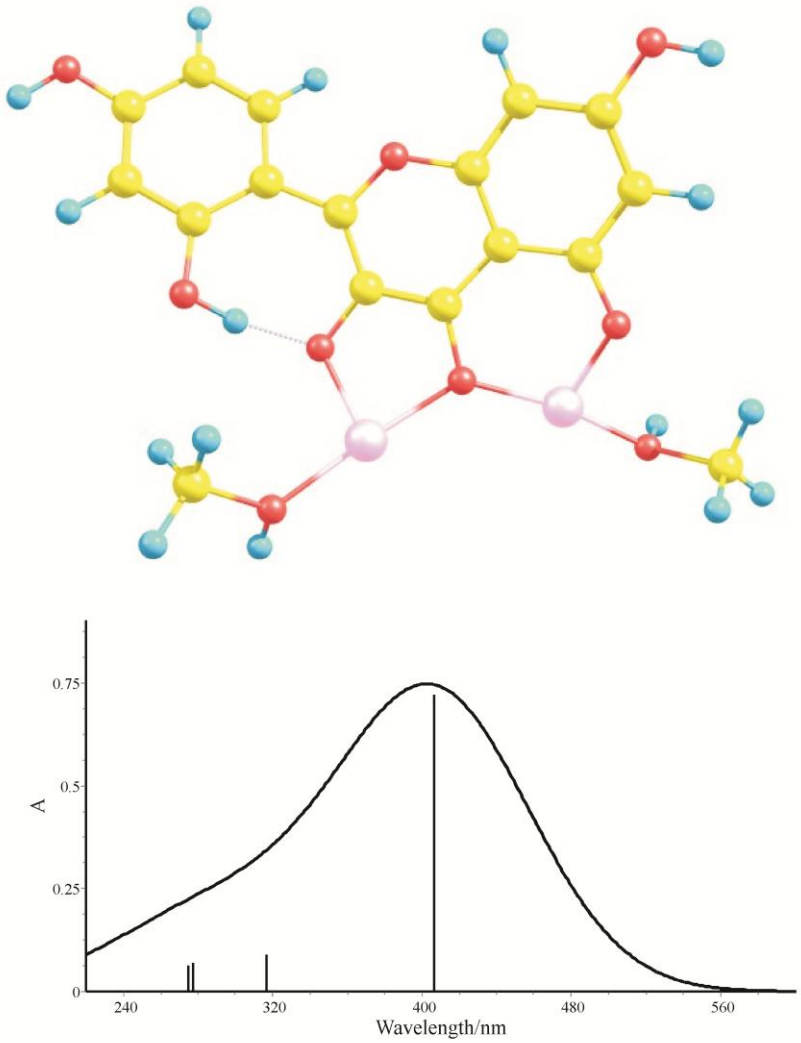

Fig. S4 Geometrically optimized structure of the 2:1 iron(II)-morin complex (top) and the calculated electronic spectrum of the supposed complex structure (bottom)

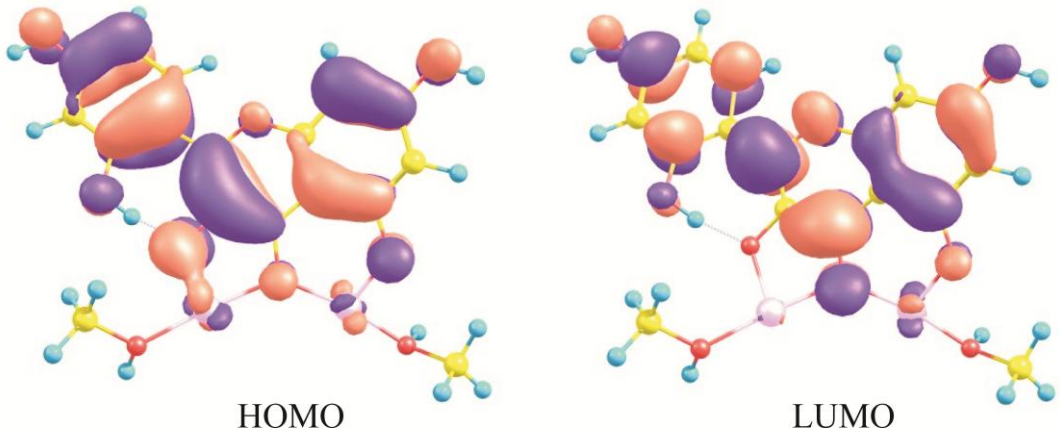

Fig. S5 The corresponding HOMO and LUMO orbitals responsible for UV-spectrum of the 2:1 iron(II)-morin complex

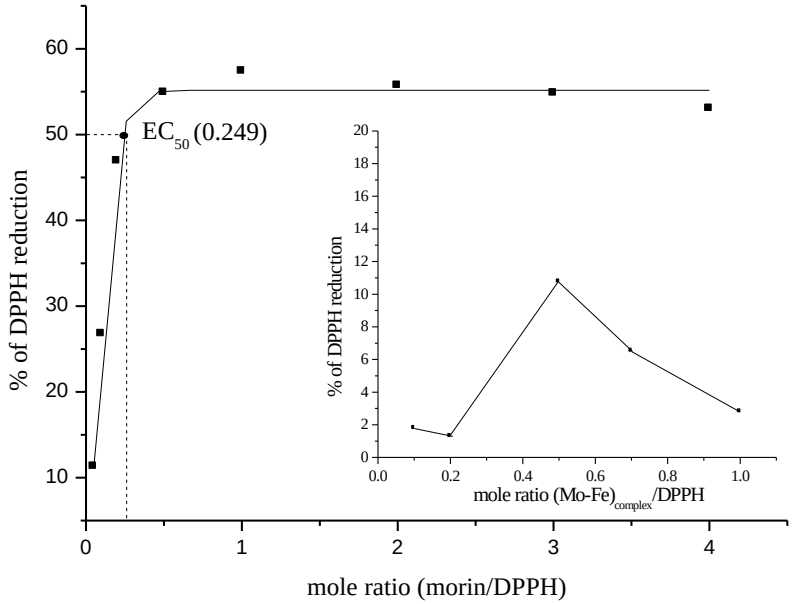

Fig. S6 Percentage of the DPPH (0.05 mM) reduction as a function of different morin/DPPH mol ratios. Inset: Percentage of DPPH reduction as a function of different (morin-Fe)/DPPH mole ratios

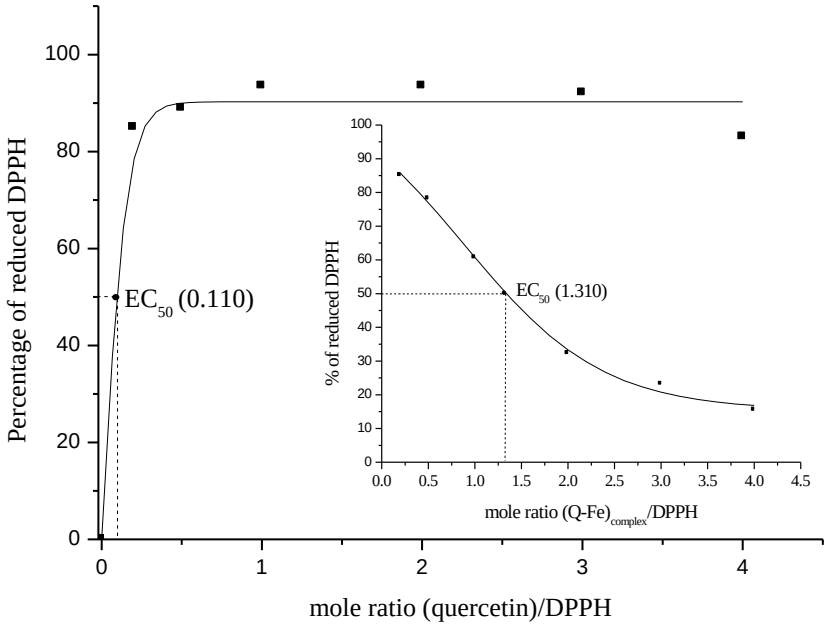

Fig. S7 Percentage of the DPPH (0.05 mM) reduction as a function of different quercetin/DPPH mole ratios. Inset: Percentage of DPPH reduction as a function of different (quercetin-Fe)/DPPH mole ratios

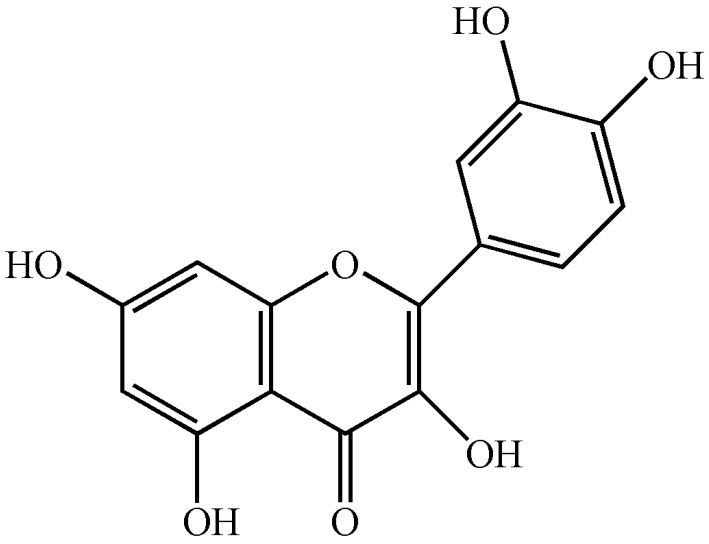

Fig. S8 Structure of quercetin

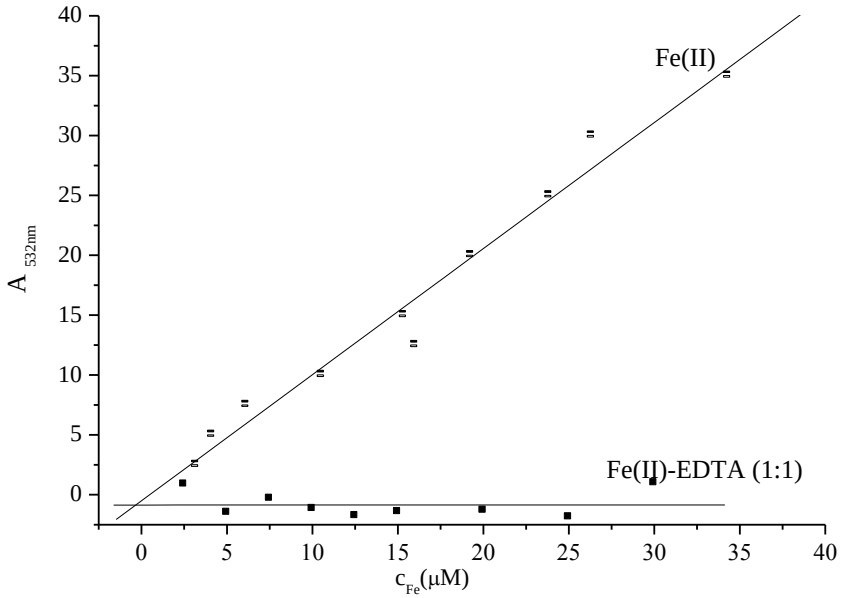

Fig. S9 Absorbance of malonaldehyde–TBA complex at 532 nm at various Fe(II) concentrations in the absence and presence of equimolar EDTA

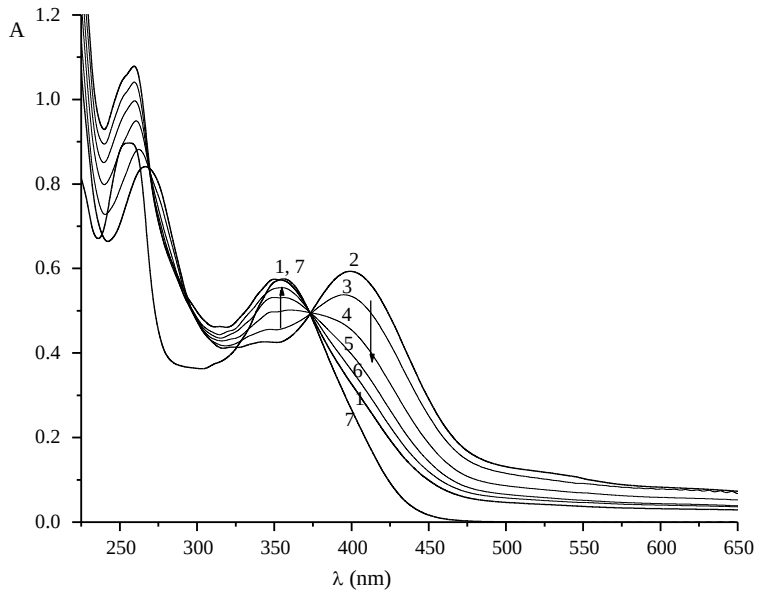

Fig. S10 Morin recovery from iron-morin complex (pH 4) by EDTA (1-morin; 2: iron-morin complex without EDTA; 3: complex + 1.0 μM EDTA; 4: complex + 1.5 μM EDTA; 5: complex + 3.1 μM EDTA 6: complex + 4.8 μM EDTA 7:complex + 6.5 mM EDTA)

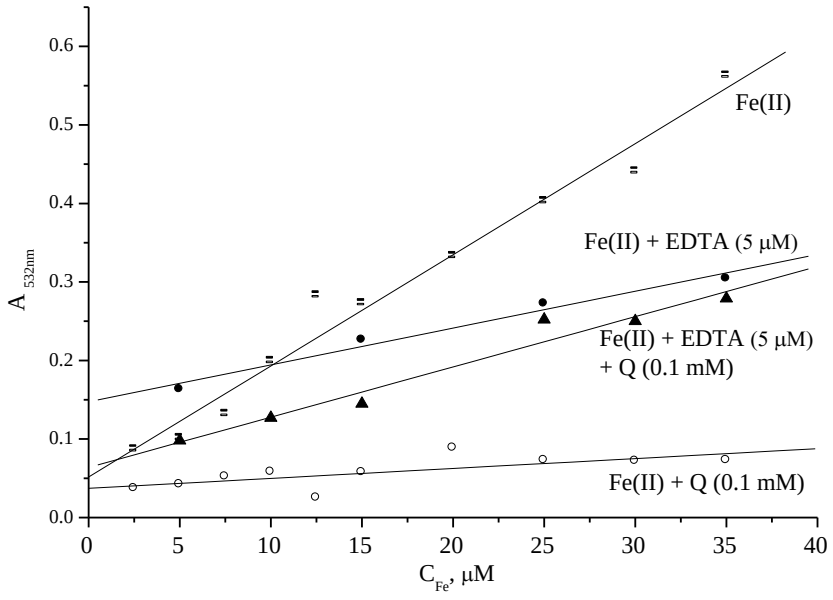

Fig. S11 Absorbance of malonaldehyde–TBA complex at 532 nm: at various Fe(II) concentrations in the presence or absence of quercetin and EDTA